2012

# Communication: Hybrid femtosecond/picosecond rotational coherent anti-Stokes Raman scattering thermometry using a narrowband time-asymmetric probe pulse

Han U. Stauffer
*Spectral Energies*

Joseph D. Miller
*Iowa State University*

Sukesh Roy
*Spectral Energies*

James R. Gord
*Air Force Research Laboratory*

# Communication: Hybrid femtosecond/picosecond rotational coherent anti-Stokes Raman scattering thermometry using a narrowband time-asymmetric probe pulse

Hans U. Stauffer, Joseph D. Miller, Sukesh Roy, James R. Gord, and Terrence R. Meyer

Citation: The Journal of Chemical Physics **136**, 111101 (2012); doi: 10.1063/1.3693669
View online: http://dx.doi.org/10.1063/1.3693669
View Table of Contents: http://scitation.aip.org/content/aip/journal/jcp/136/11?ver=pdfcov
Published by the AIP Publishing

# Communication: Hybrid femtosecond/picosecond rotational coherent anti-Stokes Raman scattering thermometry using a narrowband time-asymmetric probe pulse

Hans U. Stauffer,[1,a)] Joseph D. Miller,[2] Sukesh Roy,[1] James R. Gord,[3] and Terrence R. Meyer[2]
[1]*Spectral Energies, LLC, 5100 Springfield St., Suite 301, Dayton, Ohio 45431, USA*
[2]*Department of Mechanical Engineering, Iowa State University, Ames, Iowa 50011, USA*
[3]*Air Force Research Laboratory, Propulsion Directorate, Wright-Patterson AFB, Ohio 45433, USA*

(Received 13 January 2012; accepted 15 February 2012; published online 16 March 2012)

A narrowband, time-asymmetric probe pulse is introduced into the hybrid femtosecond/picosecond rotational coherent anti-Stokes Raman scattering (fs/ps RCARS) technique to provide accurate and precise single-shot, high-repetition-rate gas-phase thermometric measurements. This narrowband pulse—generated by inserting a Fabry-Pérot étalon into the probe-pulse beam path—enables frequency-domain detection of pure-rotational transitions. The unique time-asymmetric nature of this pulse, in turn, allows for detection of resonant Raman-active rotational transitions free of signal contamination by nonresonant four-wave-mixing processes while still allowing detection at short probe-pulse delays, where collisional dephasing processes are negligible. We demonstrate that this approach provides excellent single-shot thermometric accuracy (<1% error) and precision (~2.5%) in gas-phase environments. © *2012 American Institute of Physics*. [http://dx.doi.org/10.1063/1.3693669]

Time-resolved optical probe techniques have long been utilized as robust non-invasive diagnostics of gas-phase environments, and four-wave mixing techniques, such as coherent anti-Stokes Raman scattering (CARS), have played a crucial role in the development of increasingly sensitive and accurate temperature measurements.[1,2] As pulsed-laser technology has advanced toward higher repetition rates and shorter pulse durations—from nanoseconds (ns) to picoseconds (ps) to femtoseconds (fs)—over the past few decades, a variety of CARS techniques have been developed to take advantage of these improvements and provide accurate and precise single-shot thermometric measurements at repetition rates of 1 kHz and greater.[3] One approach that seeks to exploit simultaneously the time- and frequency-domain properties of sub-ns pulses is hybrid fs/ps CARS.[4–9] This technique, which combines two temporally overlapped broadband, fs-duration initial pulses (pump and Stokes) with a time-delayed narrowband, ps-duration final pulse (probe),[4] exhibits several advantages over other purely ps- or fs-time-resolved CARS approaches. In particular, the impulsive pump/Stokes pulses provide coherent excitation of multiple rotational[6,8] or rovibrational[5,7] transitions. The inclusion of a narrowband, ps-duration probe provides an ideal compromise of temporal and spectral resolution; the former allows detection that is outside the time window in which nonresonant (NR) components contaminate the CARS signal yet short compared to collisional decay timescales,[8] whereas the latter is necessary to observe spectrally resolved rotational or rovibrational features.

Here, we describe a unique implementation of hybrid fs/ps rotational CARS (RCARS) in which the ps-duration probe pulse is generated by placing an air-spaced Fabry-Pérot étalon in the beam path of a broadband fs-duration pulse. This produces a probe with a Lorentzian frequency-domain line shape narrow enough to resolve rotational transitions of gas-phase species such as nitrogen ($N_2$). Such spectral resolution, which is substantially higher than previous vibrational fs/ps CARS measurements using a Lorentzian bandpass filter,[7] is critical for single-shot RCARS thermometry.[6] This approach also represents an extremely straightforward application of the CARS optical probe technique, requiring only a single amplified ultrafast laser system with traditional optical components and delay lines. No parametric upconversion, as is required for vibrational CARS probes using nondegenerate pulses, and no 4-*f* pulse shaping configurations, used to generate the ps-duration probe pulse in most previous implementations of fs/ps CARS,[4,5,9] are required. As was recognized first in surface sum-frequency generation experiments by Lagutchev *et al.*,[10] another beneficial aspect of such a pulse is that it exhibits an asymmetric time-domain profile with a rapid (sub-ps) onset followed by a longer exponential decay—a direct result of the Fourier-transform relationship between the time-domain pulse and the corresponding frequency-domain Lorentzian line shape. Whereas a similar notch-filter-shaped asymmetric probe pulse has been used in single-beam CARS measurements of liquid-phase species,[11] the three-pulse configuration used here allows continuous adjustment of the asymmetric-probe-pulse delay. Thus, we demonstrate the benefits associated with this time-asymmetric probe pulse through example measurements of $N_2$ gas, including the ability to measure frequency-resolved rotational spectra at very short time delays (≤2 ps), allowing detec-

a)Author to whom correspondence should be addressed. Electronic mail: hans.stauffer.ctr@wpafb.af.mil.

 

tion prior to significant collisional dephasing while avoiding NR background. This is notably shorter than (1/7× to 1/3×) the delays used in previous fs/ps CARS measurements, which relied on probe-pulse amplitude-shaping schemes to create symmetric time-domain pulses with $[\mathrm{sinc}(t)]^2$ intensity profiles.[4,6,8,9] Also in contrast with previous fs/ps RCARS measurements,[6,8] a time-asymmetric probe pulse allows the temporal resolution of individual pure-rotational recurrences, enabling frequency-domain detection of interference effects associated with the evolving rotational wave packet.

The optical system and temperature-controlled cell used here have been described previously.[6] These experiments differ in the use of a time-asymmetric ps probe pulse, which is generated by insertion of a Fabry-Pérot étalon [TecOptics, free spectral range (FSR) = 250 $\mathrm{cm}^{-1}$, finesse = 45] into the probe-beam pathway to produce a spectrum with a Lorentzian linewidth (FWHM) of ~5.6 $\mathrm{cm}^{-1}$ centered at 800 nm. This linewidth allows resolution of $N_2$ rotational *S*-branch transitions yet decays on a time scale (1/*e* decay time: 0.9 ps) that is rapid compared to collisional dephasing lifetimes. Numerical simulations of the observed signals were carried out using a time-dependent CARS model that allows explicit inclusion of molecular and pulse electric-field parameters as well as interfering NR CARS signal that is observed when the probe pulse overlaps the pump/Stokes pair.[4,6] The time-asymmetric probe pulse used in these simulations is modeled as a Lorentzian line shape matching the experimental probe spectrum.

A schematic depicting the time evolution associated with this experimental approach is presented in Fig. 1. The three RCARS input pulses include two degenerate broadband fs-duration pulses, which provide excitation of several accessible rotational Raman $\Delta J = +2$ (*S*-branch) transitions. These pulses induce the resonant molecular response, $R(t)$, depicted in Fig. 1(a) for room-temperature $N_2$, that exhibits a highly periodic time-domain structure typical of RCARS transitions.[12–14] The repeating peaks correspond to fractional time scales associated with a full classical rotational period of $\tau_{\mathrm{full}} = n[2B_0c]^{-1}$, where $n$ is an integer, $c$ is the speed of light, and $B_0$ is the rigid-rotor rotational constant ($B_0$ = 1.99 $\mathrm{cm}^{-1}$ for $N_2$; $\tau_{\mathrm{full}}$ = 8.38 ps); integer multiples of quarter-rotational and half-rotational recurrences are also observed.[14] The simulated time-asymmetric probe pulse is shown in Fig. 1(b). The use of this pulse allows detection of NR-free signal at much shorter time delays, when collisional dephasing is negligible. In this case, the calculated first full recurrence at ~8.4 ps exhibits a ~15% intensity decay relative to the purely resonant response at $t = 0$ under 1-bar conditions [Fig. 1(a)], so measurements at partial recurrences (at 2.10 ps and 4.15 ps, for example) are necessary to reduce or remove collisional effects.

The fractional and full recurrences can be understood from a simple physical standpoint,[12] since they describe the rephasing motions of an ensemble of rotors with *J*-dependent angular frequencies $\omega_J = (1/2)J(J+1)\omega_1$, where $\omega_1 = 4\pi B_0 c$ is the fundamental rotational frequency.[12,14] The evolution of the initially prepared rotational wave packets is depicted in Figs. 1(c)–1(h) for several selected times following initiation of the $N_2$ rotational response by linearly polarized impulsive pump and Stokes

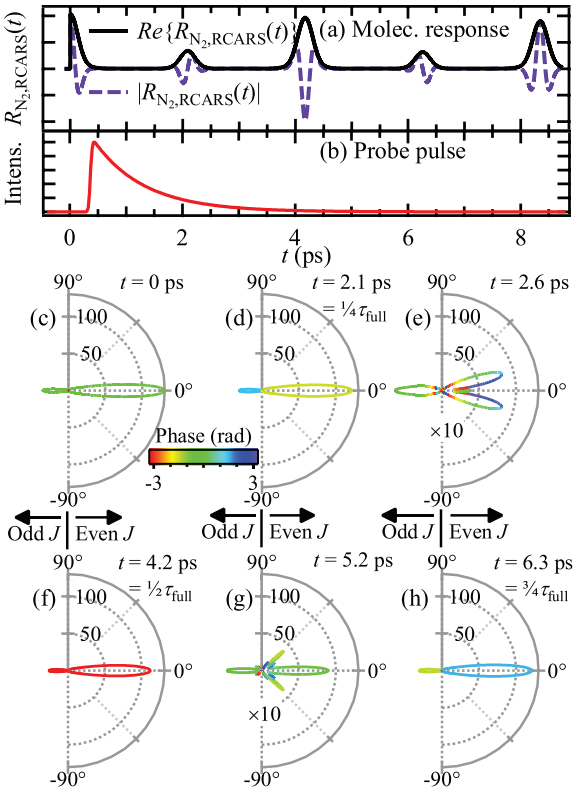


FIG. 1. (a) Time-dependent molecular response for room-temperature $N_2$ gas (*S*-branch transitions) following impulsive excitation at $t = 0$. (b) Asymmetric probe pulse shown at arbitrary delay. (c)–(h) Calculated time-dependent angular distributions associated with wave packets composed of odd-*J* and even-*J* transitions are shown for several delays. All azimuthally averaged rotational wave-packet distributions are symmetric with respect to the vertical nodal axis; only half of each distribution is shown for even-*J* (right lobes) and odd-*J* (left lobes) transitions for purpose of clarity. Radial axis depicts the amplitude of the wave packet aligned along a given laboratory angle, $\theta$, defined relative to the $\theta = 0°$ alignment of linearly polarized impulsive pump and Stokes pulses. Color scale corresponds to time-dependent accumulated phase associated with each laboratory orientation. Distributions shown in (e) and (g) are scaled 10-fold.

pulses. These together prepare an evolving superposition of states with angular alignment described by $\sum_{M=-J}^{J} \int_0^{2\pi} Y_{J+2}^M(\theta,\varphi) \cdot \cos^2\theta \cdot Y_J^M(\theta,\varphi)\, d\varphi$, where $J$ is the lower rotational state for a given *S*-branch transition [denoted *S*(*J*)], and $Y_J^M(\theta,\varphi)$ are spherical harmonics describing the $|J, M\rangle$ rotational sublevel.[14] Because even-*J* and odd-*J* transitions exhibit self-similar alignment behavior, evolving angular distributions for superpositions of even-*J* and odd-*J* states are depicted separately in Fig. 1 for illustrative purposes; the full molecular response results from a coherent sum of these two contributions. Time evolution of these coherences results from an oscillating term for each transition, $\exp[i(\omega_{J+2} - \omega_J)t]$, resulting in a time-dependent accumulated phase. Thus, the relative phase accumulation for a given *S*(*J*) transition during one full recurrence is $(4J + 6)\pi = 0$ (modulo $2\pi$), and all states within the superposition interfere constructively. At fractional ($\eta$ = 1/4, 1/2, 3/4, etc.) recurrences, each transition has an accumulated relative phase of $(4J + 6)\pi\eta$, so the relative phases of all transitions at the half recurrence are equal to $(2J + 3)\pi = \pi$ (modulo $2\pi$) for both even and odd *J* [Fig. 1(f)]. At the quarter recurrence

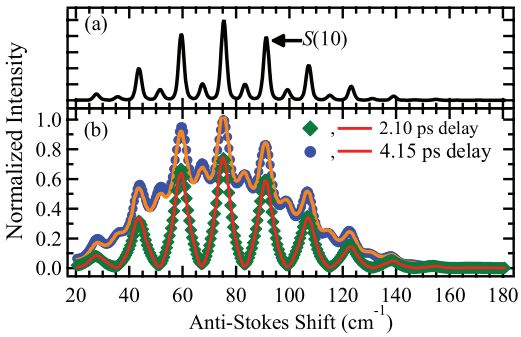


FIG. 2. (a) Simulated frequency-resolved $N_2$ rotational CARS spectrum at 298 K. (b) Experimental (symbols) and simulated (curves) $N_2$ spectra at two delays, including the first quarter-rotational (2.10-ps) and the first half-rotational (4.15-ps) recurrence.

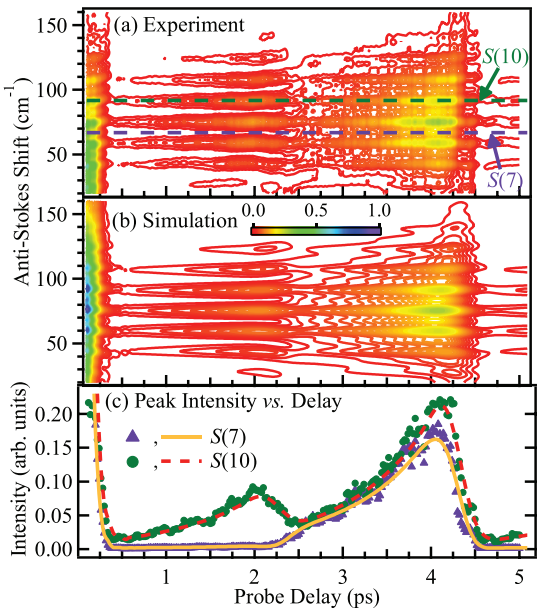


FIG. 3. Contour plots of experimental (a) and simulated (b) hybrid fs/ps RCARS data *vs.* probe delay. (c) Experimental (symbols) and simulated (curves) $S(7)$ and $S(10)$ peak intensities *vs.* probe delay.

[Fig. 1(d)], $S$-branch lines all accumulate a relative phase of $(J + 3/2)\pi$; thus, all even-$J$ lines have a relative phase of $-\pi/2$ (modulo $2\pi$) and all odd-$J$ lines have a relative phase of $\pi/2$ (modulo $2\pi$). An analogous situation occurs when $\eta = 3/4$ [Fig. 1(h)], although the roles of even-$J$ and odd-$J$ transitions are reversed. These contributions would exactly destructively interfere in cases where all even and odd levels are equally populated; however, the nuclear-spin statistics associated with $N_2$ result in a 2:1 ratio for even-$J$:odd-$J$ degeneracy factors, resulting in the presence of weaker partial recurrences at odd multiples of $\tau_{\text{full}}/4$. Two additional arbitrary fractional recurrences are also included as Figs. 1(e) and 1(g), depicting the destructive interferences that occur within the molecular Raman response away from these specific fractional recurrence times.

Examples of experimental and simulated fs/ps RCARS spectra of gas-phase room-temperature $N_2$, obtained using this time-asymmetric probe pulse, are shown in Fig. 2. As a reference, a simulated spectrum is shown in Fig. 2(a) depicting the anti-Stokes-shifted $S$-branch line positions and intensities expected for a purely frequency-resolved room-temperature $N_2$ RCARS spectrum. This simulation assumes a time-asymmetric probe pulse with a duration exactly 16 times that of the experimental probe (i.e., Lorentzian FWHM linewidth = 0.37 $\text{cm}^{-1}$; $1/e$ decay time: 14.4 ps), which results in a frequency-domain spectrum that exhibits well-separated rotational lines; however, since this simulated probe pulse spans multiple recurrences, the simulated signal exhibits nearly no temporal dependence. One reference peak is labeled $S(10)$, corresponding to the $J = 12 \leftarrow J = 10$ Raman transition; the alternating peak intensity pattern observed here results from the even $J$:odd $J$ ratio discussed above and the fact that CARS signal intensities are proportional to the square of the molecular number density.[3] Two time-dependent fs/ps RCARS spectra, measured at 2.10-ps (quarter-rotational recurrence) and 4.15-ps (half-rotational recurrence) delays, are shown in Fig. 2(b). These spectral profiles are observed to repeat nearly identically during the third quarter-rotational recurrence and the first full recurrence, respectively. Although there are obvious differences between these two observed spectra, it is important to note that the probe-pulse linewidth is sufficient to resolve discrete rotational lines at both delays. The most notable contrast between these two spectra is the absence of the odd-$J$ $S$-branch lines in the 2.10-ps results. Additionally, although both even- and odd-$J$ peaks are present in the 4.15-ps spectrum, a broad background is also observed. This background results from the fact that the probe-pulse bandwidth (5.6 $\text{cm}^{-1}$) is comparable to the rotational line spacing, $4B_0 \sim 8\ \text{cm}^{-1}$, giving rise to constructive interference between the Lorentzian-line-shape wings of each individual peak. Most notably, this background does not result from NR contributions to the observed signal, as evidenced both by the absence of obvious NR contribution to the earlier 2.10-ps probe-delay signal and by the fact that the simulated spectra included in Fig. 2(b), each containing no NR contribution, exhibit excellent agreement at both of these delays.

To explore further the probe-pulse-delay dependence observed in the CARS signal, additional fine-step time-dependence measurements were made over the 0–5 ps time scale (Fig. 3). Figures 3(a) and 3(b) show, respectively, experimental and simulated contour plots of the time-dependent CARS signal measured using this time-asymmetric probe pulse. Excellent agreement is observed, with the exception of the 0–250 fs time window, during which significant NR contributions exist and are typically difficult to model accurately. The time dependence of representative spectrally resolved odd-$J$ [$S(7)$] and even-$J$ [$S(10)$] lines are shown in Fig. 3(c). It is notable that both even- and odd-$J$ lines exhibit peaks associated with the half-rotational recurrence at 4.19 ps, yet the quarter-rotational recurrence peak is only observed in even-$J$ lines. Because the narrowband frequency-domain nature of the probe pulse allows discrete observation of individual $S$-branch transitions, each transition evolves with the relative accumulated rotational phase associated with the two $\Delta J = 2$ contributing states, as discussed above. At the half-rotational recurrence, all even and odd $S$-branch lines contain states with accumulated phases differing by odd multiples of $\pi$, resulting in a recurrence in each peak that is exactly in phase with each

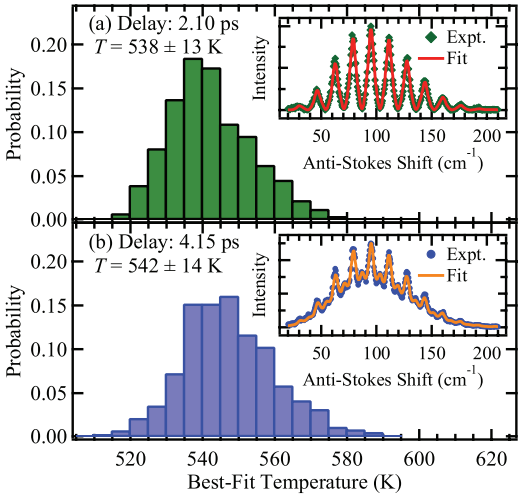


FIG. 4. Probability distribution functions for 1000 single-shot best-fit temperature measurements of $N_2$ at $T = 540$ K. (a) Probe delay = 2.10 ps and (b) probe delay = 4.15 ps. Insets show example single-shot experimental (symbols) and best-fit simulated (curves) spectra.

adjacent peak. At the quarter recurrence, in contrast, even-$J$ $S$-branch lines have accumulated relative phases of $-\pi/2$ (modulo $2\pi$), whereas odd-$J$ lines have accumulated relative phases of $\pi/2$ (modulo $2\pi$); each $S$-branch line is exactly out-of-phase with each adjacent peak. The frequency-domain resolution dictated by the chosen linewidth of the probe pulse results in the partial overlap of these adjacent lines, resulting in essentially a complete destructive interference of the weaker odd-$J$ transitions at the quarter-rotational recurrence.

Because the intended application of this time-asymmetric probe approach to fs/ps RCARS is for high-repetition-rate thermometry in low-temperature combustion environments, it is important to note the accuracy and precision associated with single-shot measurements at these two delays, particularly given the fact that the observed spectra at these two delays are notably different. One thousand single-shot spectra were recorded in a heated-cell environment ($T = 540$ K) at both the quarter- and half-rotational recurrence delays. Following optimization of several laser-dependent parameters using room-temperature $N_2$ spectra, least-squares fits to temperature-dependent simulated spectra were carried out for each single-shot spectrum in the time series. The resultant probability distribution functions and example fit single-shot spectra for each time delay are reported in Fig. 4. Excellent accuracy is observed, with corresponding precision (one-$\sigma$) of ~2.5%, independent of the choice of partial recurrence; the absence of odd-$J$ rotational lines at the shorter-delay (2.10-ps) recurrence does not reduce the temperature precision. This is particularly important under turbulent conditions that are typically encountered in real-world high-pressure combustion environments, where collisional dephasing time scales become comparable to these probe delay times and local species number densities are unknown or fluctuating, necessitating short-delay measurements. Experiments are currently underway to explore directly the ability of this time-asymmetric probe fs/ps CARS approach to detect important combustion species in high-pressure environments, both in single-species conditions and in mixtures.

Funding was provided, in part, by the National Science Foundation (NSF) (CBET-1056006, Dr. Arvind Atreya, Program Official), the Air Force Office of Scientific Research (Dr. Enrique Parra, Program Manager), and the Air Force Research Laboratory (AFRL) under Contract No. FA8650-10-C-2008. J.D.M. was supported by the National Science Foundation Graduate Fellowship Program.

[1] A. C. Eckbreth, *Laser Diagnostics for Combustion Temperature and Species* (Gordon and Breach, New York, 1996).
[2] T. Lang, M. Motzkus, H. M. Frey, and P. Beaud, J. Chem. Phys. **115**, 5418 (2001).
[3] S. Roy, J. R. Gord, and A. K. Patnaik, Prog. Energy Combust. Sci. **36**, 280 (2010).
[4] B. D. Prince, A. Chakraborty, B. M. Prince, and H. U. Stauffer, J. Chem. Phys. **125**, 044502 (2006).
[5] J. D. Miller, M. N. Slipchenko, T. R. Meyer, H. U. Stauffer, and J. R. Gord, Opt. Lett. **35**, 2430 (2010).
[6] J. D. Miller, S. Roy, M. N. Slipchenko, J. R. Gord, and T. R. Meyer, Opt. Express **19**, 15627 (2011).
[7] J. D. Miller, M. N. Slipchenko, and T. R. Meyer, Opt. Express **19**, 13326 (2011).
[8] J. D. Miller, C. E. Dedic, S. Roy, J. R. Gord, and T. R. Meyer, Opt. Express **20**, 5003 (2012).
[9] D. Pestov, R. K. Murawski, G. O. Ariunbold, X. Wang, M. C. Zhi, A. V. Sokolov, V. A. Sautenkov, Y. V. Rostovtsev, A. Dogariu, Y. Huang, and M. O. Scully, Science **316**, 265 (2007).
[10] A. Lagutchev, S. A. Hambir, and D. D. Dlott, J. Phys. Chem. C **111**, 13645 (2007).
[11] O. Katz, J. M. Levitt, E. Grinvald, and Y. Silberberg, Opt. Express **18**, 22693 (2010).
[12] P. M. Felker, J. Phys. Chem. **96**, 7844 (1992).
[13] H. M. Frey, P. Beaud, T. Gerber, B. Mischler, P. P. Radi, and A. P. Tzannis, Appl. Phys. B: Lasers Opt. **68**, 735 (1999).
[14] P. W. Dooley, I. V. Litvinyuk, K. F. Lee, D. M. Rayner, M. Spanner, D. M. Villeneuve, and P. B. Corkum, Phys. Rev. A **68**, 023406 (2003).